

MULTIGRID ACCELERATION OF THREE-DIMENSIONAL TURBULENT, VARIABLE-DENSITY FLOWS

P. A. Rubini

Departments of Mechanical and Chemical Engineering, Queen's University, Kingston, Ontario K7L 3N6, Canada

H. A. Becker and E. W. Grandmaison

Department of Chemical Engineering, Queen's University, Kingston, Ontario K7L 3N6, Canada

A. Pollard

Department of Mechanical Engineering, Queen's University, Kingston, Ontario K7L 3N6, Canada

A. Sobiesiak and C. Thurgood

Departments of Mechanical and Chemical Engineering, Queen's University, Kingston, Ontario K7L 3N6, Canada

Multigrid acceleration is applied to a finite-volume method for the calculation of three-dimensional, variable-density turbulent flow. Turbulence is modeled by the k- ϵ model with the transport equations incorporated into the multigrid procedure. Density variations are fully accounted for. A full approximation multigrid method is developed using mass-conserving restriction and prolongation operators. A significant reduction in overall computing time is shown for both constant-density and variable-density flow over a three-dimensional backward-facing step. It is concluded that the method is suitable for application to complex three-dimensional flows of practical engineering interest.

INTRODUCTION

Turbulence and variable density occur in many low-Mach-number flows of industrial importance, perhaps most commonly in those with heat transfer and combustion. Consequently, there has been a significant development of computational fluid dynamics (CFD) techniques aimed at solving flows of this type (see, for example, Jones and Whitelaw [1]). In general, the numerical solution of the equations governing such problems is accomplished using iterative techniques that have little regard for computer time or cost. Typically, the computational time is proportional to the square of the number of grid nodes. As a result, the application of CFD to turbulent, variable-density flows is frequently limited either by time or by the largest grid size whose solution may be obtained within a given cost.

The financial support of the Natural Sciences and Engineering Research Council of Canada, the Ministry of Energy of Ontario, and the Ferrous Industry Energy Research Association is gratefully acknowledged. P. A. Rubini is now at Cranfield Institute of Technology, England.

NOMENCLATURE			
A	control volume face area , m^2	x_i	Cartesian spatial coordinate
A_p, A_f, S	algebraic coefficients	δ_{ij}	Kronecker delta
C_{μ}, C_1, C_2	turbulence model constants	ϵ	rate of dissipation of turbulent energy , m^2/s^3
S_i	Cartesian component of gravitational force, m/s^2	ϵ	multigrid source term
I	intergrid transfer operator	η	smoothing rate
k	specific kinetic energy of turbulence, m^2/s^2	μ	dynamic viscosity, $N\ s/m^2$
M_α	molar mass of species α , $kg/kmol$	μ_t	turbulent viscosity, $N\ s/m^2$
P	pressure, N/m^2	ϕ	general variable
r^k	solution residual error on grid k	φ	scalar variable
R	gas constant ($-8.314\ kJ/kmol\ K$)	ρ	density, kg/m^3
T	temperature, K	σ_ϕ	Prandtl/Schmidt number for variable ϕ
U_i	Cartesian mean velocity component, m/s	τ	shear stress, N/m^2
u_i	Cartesian fluctuating velocity component, m/s	Superscripts	
w_α	mass fraction of species a	\sim	density-weighted , or Favre, average
		$-$	time average

The technique of multigrid acceleration has been applied by a number of authors to fluid flow problems [2-7]. Savings in computer time of over an order of magnitude have been reported when the technique is compared with conventional single-grid techniques. Originally devised for linear boundary-value problems, the technique has been further developed for nonlinear partial differential equations such as the Navier-Stokes equations [8]. However, most problems examined have been restricted to two-dimensional laminar flows with constant properties. Only recently has the technique been extended to more complex geometries and flows. Joshi and Vanka [9] incorporated a multigrid algorithm into a general curvilinear code for two-dimensional geometries. Vaughan et al. [10] applied a multigrid procedure to the flow between rotating disks, using a mixing length turbulence model. Yokota [11] developed a multigrid algorithm for compressible flows, incorporating the k - ϵ turbulence model. Peric et al. [12] applied a multigrid procedure to two-dimensional flow over a backstep, also using the k - ϵ turbulence model.

This article further develops the application of multigrid acceleration to three-dimensional variable-density turbulent flow. Turbulence is modeled using the two-equation k - ϵ model, and large density variations are **allowed**. Results are presented for flow over a three-dimensional, backward-facing **step**.

GOVERNING EQUATIONS

The **Favre-averaged**, steady-state governing equations in Cartesian tensor notation are given by

$$\frac{\partial}{\partial x_i}(\bar{\rho}\tilde{U}_i) = 0 \quad (1)$$

$$\frac{\partial}{\partial x_j} (\bar{\rho} \tilde{U}_i \tilde{U}_j) = -\frac{\partial \bar{P}}{\partial x_i} + \frac{\partial}{\partial x_j} (\bar{\tau}_{ij} - \bar{\rho} \tilde{u}_i \tilde{u}_j) + \rho g_i \quad (2)$$

$$\frac{\partial}{\partial x_j} (\bar{\rho} \tilde{U}_i \tilde{\varphi}) = \frac{d}{dx_j} \left(\frac{\mu}{\sigma_\varphi} \frac{d\tilde{\varphi}}{dx_j} - \bar{\rho} \tilde{u}_i \tilde{\varphi} \right) \quad (3)$$

$$\bar{\tau}_{ij} = \mu \left(\frac{\partial \tilde{U}_i}{\partial x_j} + \frac{\partial \tilde{U}_j}{\partial x_i} - \frac{2}{3} \delta_{ij} \frac{\partial \tilde{U}_k}{\partial x_k} \right) \quad (4)$$

where $U_i = \bar{U}_i + u_i$, $\tilde{U}_i = \bar{\rho} U_i / \bar{\rho}$, etc., and where the turbulence correlations (e.g., $\tilde{u}_i \tilde{u}_j$) imply density weighting in the usual manner [1].

The turbulent shear stresses are modeled through the two-equation k - ϵ turbulence model, in the form given by Launder and Spalding [13]. The shear stresses are related to the mean rate of strain by

$$\bar{\rho} \tilde{u}_i \tilde{u}_j = \frac{2}{3} \delta_{ij} \left(\bar{\rho} k + \mu_t \frac{\partial \tilde{U}_k}{\partial x_k} \right) \sim \mu_t \left(\frac{\partial U_i}{\partial x_j} + \frac{\partial U_j}{\partial x_i} \right) \quad (5)$$

The turbulence viscosity is modeled by

$$f\mu = C_\mu \bar{\rho} \frac{k^2}{\epsilon} \quad (6)$$

where k and ϵ represent the turbulent kinetic energy and the rate of dissipation of turbulent kinetic energy, respectively. The turbulent scalar flux is approximated by the gradient diffusion model

$$\bar{\rho} \tilde{u}_i \tilde{\varphi} = -\frac{\mu_t}{\sigma_\varphi} \frac{\partial \tilde{\varphi}}{\partial x_i} \quad (7)$$

The k - ϵ turbulence model requires that a transport equation be solved for each variable, as follows:

$$\text{to y} \frac{d}{dx_j} (\bar{\rho} U_i k) = \frac{d}{dx_j} \left[\left(\mu + \frac{\mu_t}{\sigma_k} \right) \frac{\partial k}{\partial x_j} \right] - \bar{\rho} \tilde{u}_i \tilde{u}_j \frac{\partial U_i}{\partial x_j} - \bar{\rho} \epsilon \quad (8)$$

$$\frac{\partial}{\partial x_j} (\bar{\rho} \tilde{U}_i \epsilon) = \frac{\partial}{\partial x_j} \left[\left(\mu + \frac{\mu_t}{\sigma_\epsilon} \right) \frac{\partial \epsilon}{\partial x_j} \right] - C_1 \frac{\epsilon}{k} \bar{\rho} \tilde{u}_i \tilde{u}_j \frac{\partial \tilde{U}_i}{\partial x_j} - C_2 \bar{\rho} \frac{\epsilon^2}{k} \quad (9)$$

The constants in the above equations have been assigned the empirical values of Launder and Spalding [13]; however, for internal flows these are not optimum [14]. Buoyancy effects are not included in the turbulence model.

The fluid is supposed incompressible. However, the density varies with temperature and composition. This is accounted for by employing density-weighted averaging of the conservation equations according to the ideal gas law,

$$\rho = \frac{P}{RT \sum_n (w_\alpha / M_\alpha)} \quad (10)$$

The local density, for an assumed two-component system, should be calculated from

$$\frac{1}{\rho} = \left(\frac{w_1}{\rho_1 T_1} + \frac{w_2}{\rho_2 T_2} \right) (w_1 T_1 + w_2 T_2) \quad (11)$$

where w are the local mass fractions and the subscripts refer to components a in Eq. (10). Equation (11) assumes constant fluid specific heats; however, the problem considered here is to demonstrate the multigrid method and so the following approximation to Eq. (11) is used:

$$p = \varphi \rho_1 + (1 - \varphi) \rho_2 \quad (12)$$

where ρ_1 and ρ_2 represent the densities corresponding to hot or cold fluid, respectively. The scalar variable φ in Eq. (12) is calculated from Eq. (3) and Eq. (7) with the Prandtl/Schmidt number assumed equal to unity and $0 < \varphi < 1$.

NUMERICAL METHOD

Multigrid Acceleration

The basic principle of multigrid acceleration is to increase the rate of information transfer during the iterative solution of a set of algebraic equations over a discretized solution domain. Analysis has shown that the performance of commonly used numerical techniques dramatically degrades as the grid density is increased. Fourier analysis reveals that such techniques are most efficient at removing errors at wavelengths comparable to the mesh size and are inefficient at wavelengths much greater than the mesh size. Therefore, solving a given problem simultaneously on a number of successively coarser coincident grids should enhance the overall rate of information transfer and hence the rate of error reduction, provided that suitable intergrid transfer operators are employed. A detailed analysis of the multigrid procedure is given by Brandt [8]. Shaw and Sivaganathan [15] present an analysis of the smoothing properties of the SIMPLE [16] algorithm, a variant of which is used in the present work. Details of the nonlinear multigrid algorithm used in this study are given below.

The final form of the algebraic equations, after discretization and linearization of the governing equations of motion, is

$$A_p \phi_p - \sum_i A_i \phi_i + S \quad (13)$$

where the summation is over the adjacent nodes utilized during the discretization procedure. The assembly and solution of this equation set on any given grid is called smoothing in multigrid terminology. During the iterative solution of the above equation set on a fine grid k , Eq. (13) becomes:

$$A_p^k \phi_p^k - \sum_i \phi_i^k + S^k + r^k \quad (14)$$

where r^k represents the current solution error on grid k . Once the residual reduction rate falls below a prescribed value $\eta = R_{i+1}/R_i$, where R_i is some norm of the residual error on the i th iteration, the solution is transferred to a coarser grid, $k + 1$. On this grid,

$$A_p^{k+1} I_k^{k+1} \phi_p^k = \sum_i A_i^{k+1} I_k^{k+1} \phi_i^k + S^{k+1} + I_k^{k+1} r^k + \epsilon \quad (15)$$

where I_k^{k+1} is an intergrid transfer operator from grid k to grid $k + 1$ and ϵ is the resultant error on the grid $k + 1$. For a converged solution, ϵ is the error on grid $k + 1$ arising from applying the smoothing scheme to a coarser grid.

The solution on grid $k + 1$ is smoothed for a number of iterations, giving an improved solution

$$A_p^{k+1} \phi_p^{k+1} = \sum_i A_i^{k+1} \phi_i^k + S^{k+1} + \epsilon + r^{k+1} \quad (16)$$

where

$$\epsilon = A_p^{k+1} I_k^{k+1} \phi_p^{k+1} - \sum_i A_i^{k+1} I_k^{k+1} \phi_i^k - S^{k+1} - I_k^{k+1} r^k \quad (17)$$

As a result of applying the smoothing to the coarse grid, the solution is improved. A correction to the original interpolated fine-grid solution is then obtained:

$$\phi_{\text{correction}}^{k+1} = \phi^{k+1} - I_k^{k+1} \phi^k \quad (18)$$

Finally, the correction is transferred to the fine grid, thereby completing one two-grid, multigrid V-cycle. The full potential of the multigrid procedure may be realized by providing several successively coarser grids such that the whole range of error components is smoothed.

Several strategies are possible [17] for cycling between the solution grids. In the present study a variant of the full multigrid (FMG) algorithm is employed. In FMG, the solution to the discretized equations is obtained on a given grid k , typically using a V-cycle multigrid procedure, starting from the prolonged values of a converged solution on the next coarser grid $k + 1$. This procedure is applied recursively to all coarser grids and results in a converged solution on all previous grids as an initial estimate for the next finer grid.

In the present work, the FMG algorithm was found to be inefficient for turbulent three-dimensional flows; therefore, a converged solution was obtained on only the coarsest grid, whereupon a conventional V-cycle was followed. The smoothing factor η was set at 0.95 on the coarsest grid and 0.8 on all finer grids, based on the sum of the absolute mass errors over all control volumes.

Finite-Volume Smoothing Algorithm

The governing equations are integrated and **discretized** using an elliptic finite-volume procedure and a staggered velocity-storage arrangement. The SIMPLE pressure correction algorithm, in the form suggested in Ref. [18], is used to close the set of algebraic equations. The resultant equations are solved for each solution variable in turn using a line **Gauss-Seidel** solver. **Underrelaxation** is necessary due to the coupled nonlinear nature of the equations and is carried out implicitly via the coefficients (0.3 for momentum, **1.0** for passive **scalars**, 0.5 for k and ϵ). No underrelaxation is required for pressure, density, or turbulent viscosity. Typically, one sweep of the solver is used for all solution variables except the pressure correction, for which six sweeps are used. A fixed number of solver sweeps was adopted for simplicity. **Latimer** and Pollard [19] have investigated an adaptive strategy in which the number of solver sweeps is controlled by the rate of residual reduction.

Boundary conditions are required on all surfaces of the solution domain. The present computer code has been developed to allow for the arbitrary location of fixed-value (inlet/exit), symmetry, and **extrapolative** gradient boundary conditions. The mean velocity and turbulence profiles adjacent to a **solid** wall are defined by **semiempirical** relationships derived from the logarithmic law of the wall [13].

Restriction

Figure 1 illustrates the variable-storage arrangement adopted in the present study. While the grid may be **nonuniform**, scalar variables are stored at the center of the control

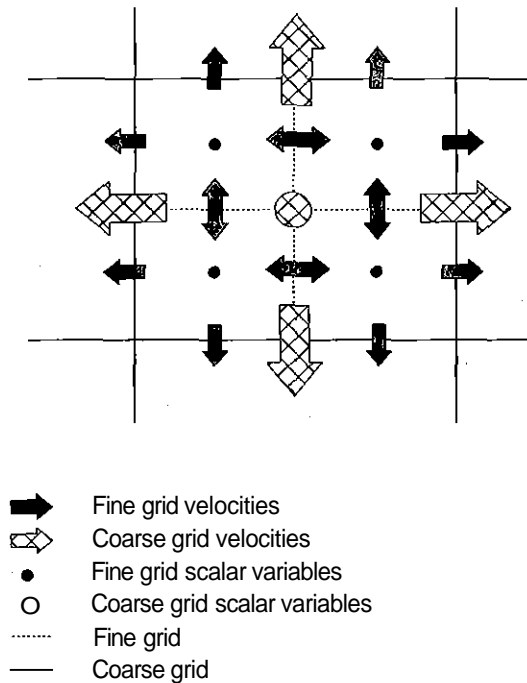


Fig. 1 Finite-volume variable storage.

Density
2.450E-01
2.950E-01
3.450E-01
3.950E-01
4.450E-01
4.950E-01
5.450E-01
5.950E-01
6.450E-01
6.950E-01
7.450E-01
7.950E-01
8.450E-01
8.950E-01
9.450E-01
9.950E-01
1.045E+00

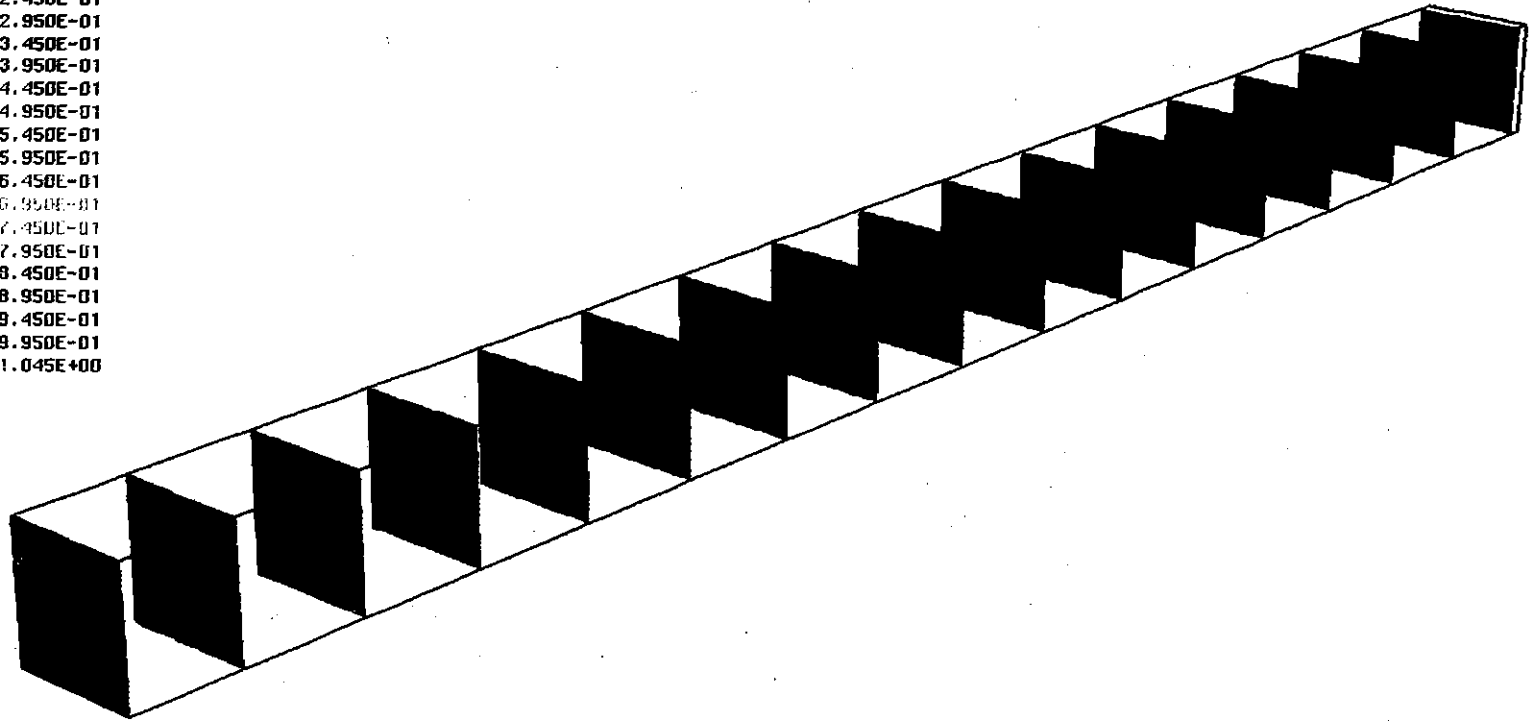


Fig. 5 Density field, variable-density flow.



volume and velocities are stored at the center of a control-volume face. Grid refinement is achieved by subdividing coarse-grid control volumes. The process of control-volume subdivision is consistent with the integral approach used to derive the finite-volume algorithm and provides a simple means to ensure mass conservation. Sivaloganathan and Shaw [5] derived a similar approach, which they termed "continuity control volume lumping." Although mass conservation between individual grids may not be necessary in a **multigrid** context, it is essential in the context of an embedded **multigrid/multilevel** technique for variable-density flows [20].

Mass conservation requires that, on an individual control-volume face,

$$(\rho UA)_{\text{coarse}} = \sum_{\text{fine}} (\rho UA) \quad (19)$$

where the summation is over all fine-grid control-volume faces coincident with the coarse-grid face. Therefore the coarse-grid face velocity may be defined as

$$U_{\text{coarse}} = \frac{\sum_{\text{fine}} (\rho UA)}{(\rho A)_{\text{coarse}}} \quad (20)$$

Equation (20) requires that the coarse-grid density be known. This is achieved by restricting the solution variables that determine the density, taken here as a single passive scalar, prior to restricting the velocities. The density is evaluated on the coarse grid using the restricted fine-grid values. Restriction of solution variables stored at the control-volume node is achieved by three-dimensional linear interpolation between the fine-grid subcontrol volumes. The solution residuals are restricted in an analogous manner. Optimum convergence was found when the momentum residuals were overrelaxed by a factor of 4, equivalent to summing the fine-grid residuals.

Prolongation

To be consistent with the restriction operator, prolongation should also be mass conserving. For variable-density flows this would be very difficult to achieve using polynomial interpolation between neighboring coarse-grid velocity nodes. Therefore mass flow corrections are directly prolonged over coincident **control-volume** faces.

Referring to Eq. (19), the net mass flow correction through a given control-volume face, arising from applying finite-volume smoothing to the coarse grid, may be expressed as

$$(\rho^* U^* A)_{\text{coarse}} - \sum_{\text{fine}} (\rho^\dagger U^\dagger A) \quad (21)$$

where the asterisk refers to the smoothed coarse-grid solution and the dagger to the updated fine-grid values. Assuming a constant velocity correction for all fine-grid sub-control volumes gives

$$\Delta U_{\text{fine}} = \left[(\rho^* U^* A)_{\text{coarse}} - \sum_{\text{fine}} (\rho^\dagger U^\dagger A) \right] / \sum_{\text{fine}} (\rho^\dagger A) \quad (22)$$

where U^o refers to the original fine-grid velocity. This procedure requires prior knowledge of the updated fine-grid density, evaluated using the corrected **values** of the appropriate solution variables. Prolongation of nodal variables is achieved by direct injection on an equal basis of the coarse grid correction into each fine-grid subvolume.

Treatment of Correction to Pressure

The **SIMPLEC** algorithm attempts to satisfy continuity on a given grid by generating pressure and velocity corrections. This is achieved by deriving a Poisson equation for the pressure correction, in which the source term is the control-volume mass error. In a multigrid cycle, the pressure is transferred between grids, but not the pressure correction. This practice ensures that continuity is independently satisfied on all grids, with a consistent pressure field. The pressure is propagated between grids using the scalar **intergrid** operators.

Multigrid Acceleration of the k - ϵ Equations

The highly nonlinear nature of the k - ϵ equations requires careful treatment within a multigrid procedure to achieve optimal convergence rates. Previous attempts have not included the k - ϵ equations within the multigrid cycle, but instead have solved for these equations on the **fine** grid and transferred only the turbulent viscosity [11, 21]. Joshi and **Vanka** [9] present some results for turbulent flow with the k - ϵ model but give no details of their procedure. The work of Peric et al. [12] represents possibly the first published application of multigrid acceleration to the k - ϵ equations.

In the present work, no special treatment of the k or ϵ boundary conditions was found necessary. However, additional linearization of the source terms was found necessary to prevent negative values of k or ϵ . To ensure positive values, Eq. (16) is rearranged in the following manner:

$$A_p^k \phi_p^k = \sum_i A_i^k \phi_i^k + S^k + \epsilon + r^k \quad \epsilon > 0$$

$$\left(A_p + \frac{\epsilon}{\phi_p} \right) \phi_p = \sum_i A_i^k \phi_i^k + S^k + r^k \quad \epsilon < 0$$
(23)

Negative values of k or ϵ can also arise during the prolongation operation in regions of large gradients. This problem was circumvented by simply not updating any locations that would result in a negative value.

PRESENTATION AND DISCUSSION OF RESULTS

The flow over a three-dimensional, backward-facing step is chosen to demonstrate the numerical procedure. The geometry produces a significant recirculation zone with a region of high shear and allows the use of **extrapolative** exit boundary conditions. Because of the high aspect ratio, numerical discretization results in control volumes with aspect ratios greater than unity and with an unequal number of control volumes in each coordinate direction. In addition, constant- and variable-density flows are considered.

The problem thus demands a robust and efficient numerical algorithm to obtain an economical solution. As the **multigrid** procedure acts only to accelerate the convergence of the underlying finite-volume procedure, the numerical results should be consistent with previous single-grid calculations, the performance of which have been extensively documented [18, 19]. Therefore no comparison is made with experimental data.

Figure 2 shows the backstep geometry, with step height $h = 0.25$ m. The inlet Reynolds number $Re (= \rho U h / \mu)$ was set to 1×10^5 , and the inlet mass flow m was 0.125 kg/s. Profiles of all variables were taken as uniform at the inlet with turbulence intensity $\sqrt{k}/U_{inlet} = 0.015$ and turbulence length scale $X - h = 0.25$ m, where $\epsilon = 0.09k^{3/2}/\lambda$.

The calculations were commenced with a zero mean velocity field and a turbulence field initialized to the inlet values. Calculations were continued until the sum of the absolute values of the local control-volume mass errors, normalized by the inlet mass flow, was less than 10^{-4} . All calculations were performed on a Silicon Graphics 4D/240/GTX workstation with 64 MB of memory. The code was run on a single processor only.

Variable-density calculations were done for an asymmetric inlet profile of the passive scalar shown in Fig. 2. The two halves of the profile were defined as $\phi = 0$ and $\phi = 1$, respectively, with corresponding reference densities defined as $\rho_1 = 0.25$ and $\rho_2 = 1.0$.

Calculations were carried out on **five** grids, with each successively finer grid representing a doubling of the number of control volumes in each coordinate direction. A total of $128 \times 32 \times 32$ control volumes were utilized on the finest grid, with a resultant aspect ratio of **4:1** in the axial direction. Results were obtained for both constant density and variable density. Results for the finest grid were not obtained using a single grid due to the projected excessive computing time.

Figure 3 presents contours of axial velocity along the solution domain for constant-

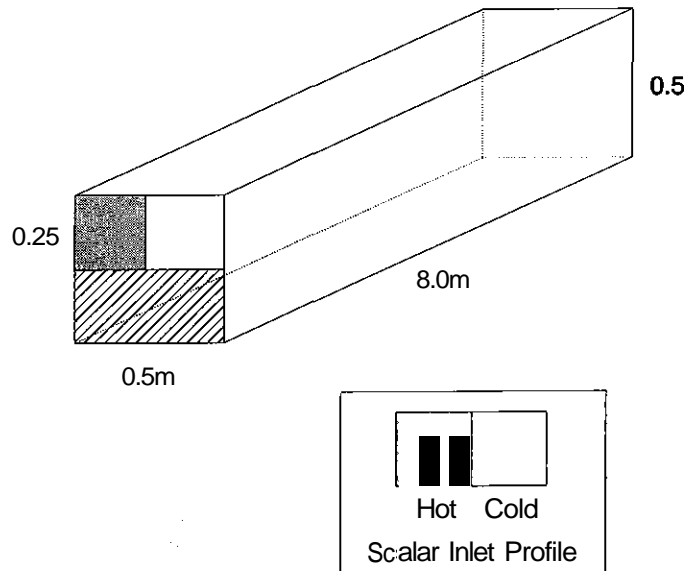


Fig. 2 **Three-dimensional** backstep including passive scalar inlet profile.

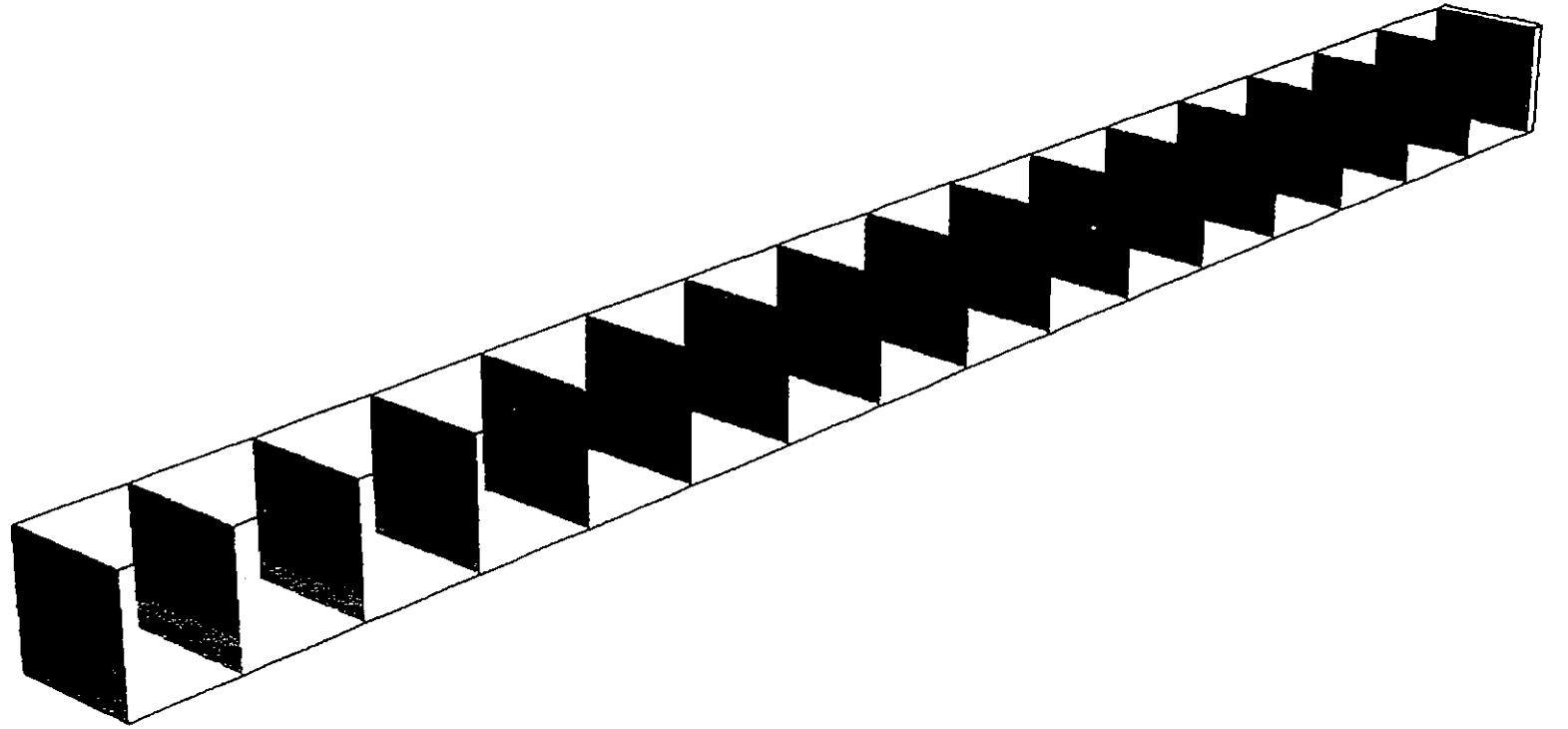


Fig. 3 Axial **velocity** contours, constant-density flow.

density flow. The region of **recirculation** is visible downstream of the backstep, beyond which the flow slowly recovers to an almost fully developed profile. Figures 4 and 5 present the results for variable-density flow (see color plate for Fig. 5). The variable-density flow is significantly different, with a considerable degree of three-dimensionality evident. Study of Fig. 4 reveals a second region of recirculation above the backstep on the hot side of the flow.

Table 1 shows the number of iterations required to obtain converged solutions for the single-grid and **multigrid** algorithms. The **single-grid** results show the usual dramatic increase in the number of iterations, whereas the **multigrid** results reveal only a modest increase.

Figure 6 presents a typical plot of the convergence histories of the $64 \times 16 \times 16$ grid using the two solution schemes. The abscissa represents fine grid work units, defined as computer time required for one iteration on the **fine** grid using the single-grid scheme. The ordinate represents the sum of the absolute local control-volume mass errors, normalized by the inlet mass flow. The mass error using the **multigrid** scheme decreases at an almost linear rate, with no oscillations.

Table 2 shows the computer time required to obtain solutions on the different grids. The results are normalized to the computer time for the coarsest ($8 \times 2 \times 2$) grid. The value for the finest grid using the single-grid technique was extrapolated from the coarse-grid results. The values are plotted in Fig. 7.

The exponents of a power-law curve fit to the slopes of the logarithmic plots are 1.32 and 1.58 for the **multigrid** and single-grid schemes, respectively. The exponent for the single-grid algorithm is lower than that quoted by previous **investigators**, 1.92 [12] and 1.65 [7]. It is believed that this is due to the relative efficiency of the alternating direction line solver when it is used for three-dimensional turbulent flows [22].

The exponent for the **multigrid** algorithm is considerably greater than unity. This is most likely related to the prolongation scheme used within the present **multigrid** procedure, which, although mass conserving, is otherwise a low-order scheme. However, the difference in the exponent between the two schemes still results in a considerable reduction in overall computing time that is estimated to be greater than a factor of 25 for the finest grid. This result compares very well with two-dimensional calculations using a grid with a similar number of control volumes [12].

All calculations were performed using the **underrelaxation** factors defined earlier, previously determined to be optimum for single-grid calculations. No attempt was made to improve the performance of the **multigrid** calculations by further optimization of the underrelaxation factors. No modifications were necessary to obtain converged solutions.

SUMMARY

The technique of **multigrid** acceleration has been successfully applied to three-dimensional, variable-density, turbulent flow over a backstep. The results indicate a dramatic reduction in the computer time required to obtain a solution, by a factor of over 25 for the finest grid considered. However, the expected linear increase of computing time with respect to number of grid nodes was not achieved. This is most likely a result of using a low-order but mass-conserving prolongation scheme.

The transport equations for the turbulence parameters k and ϵ were successfully incorporated into the **multigrid** algorithm. The scheme may therefore be readily ex-

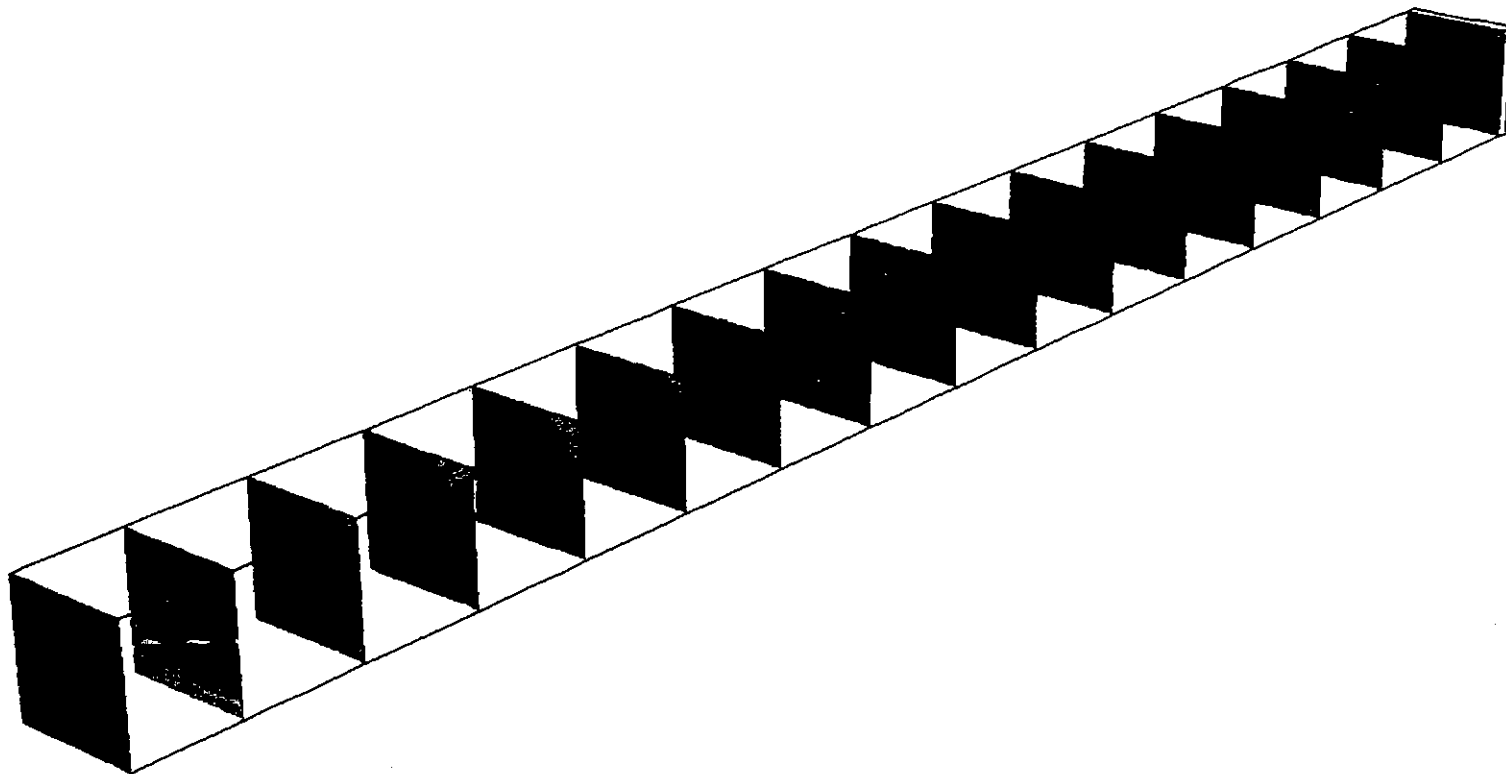


Fig. 4 Axial velocity contours, **variable-density** flow.

Table 1 Number of Iterations Required to Obtain a Converged Solution

Flow	Grid	Number of control volumes				
		32	256	2048	16384	131072
Constant density	Single grid	109	316	942	2260	
	Multigrid	109	18	20	28	43
Variable density	Single grid	102	286	682	1352	
	Multigrid	102	16	24	35	56

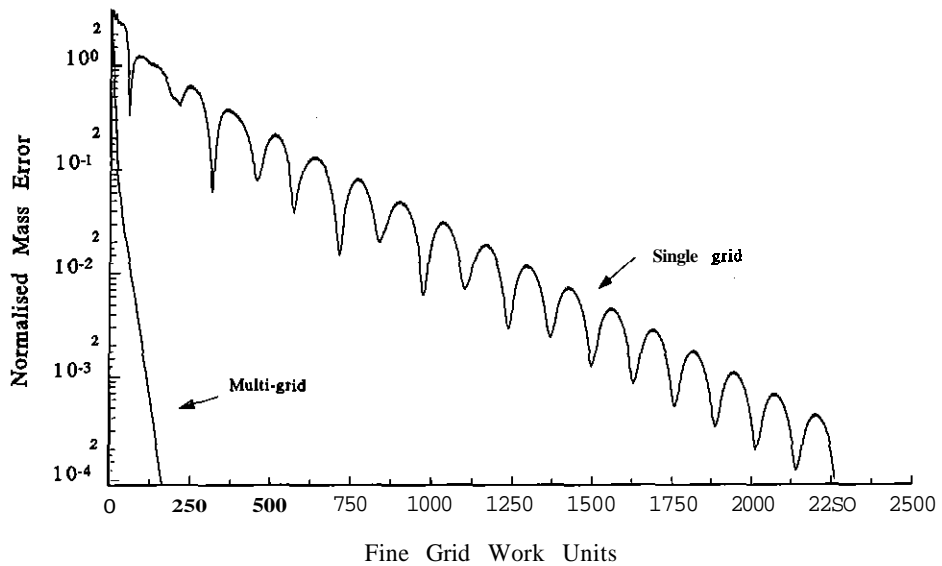


Fig. 6 Convergence history for constant-density flow on a 64 x 16 X 16 grid.

Table 2 Normalized Computer Time Required to Obtain a Converged Solution

Flow	Grid	Number of control volumes				
		32	256	2048	16384	131072
Constant density	Single grid	1	14.2	316.8	8576.3	231000 Est.
	Multigrid	1	4.5	38.9	575.7	8974.0
Variable density	Single grid	1	11.9	221.9	5499.0	136350 Est.
	Multigrid	1	4.5	52.4	830.0	13381.0

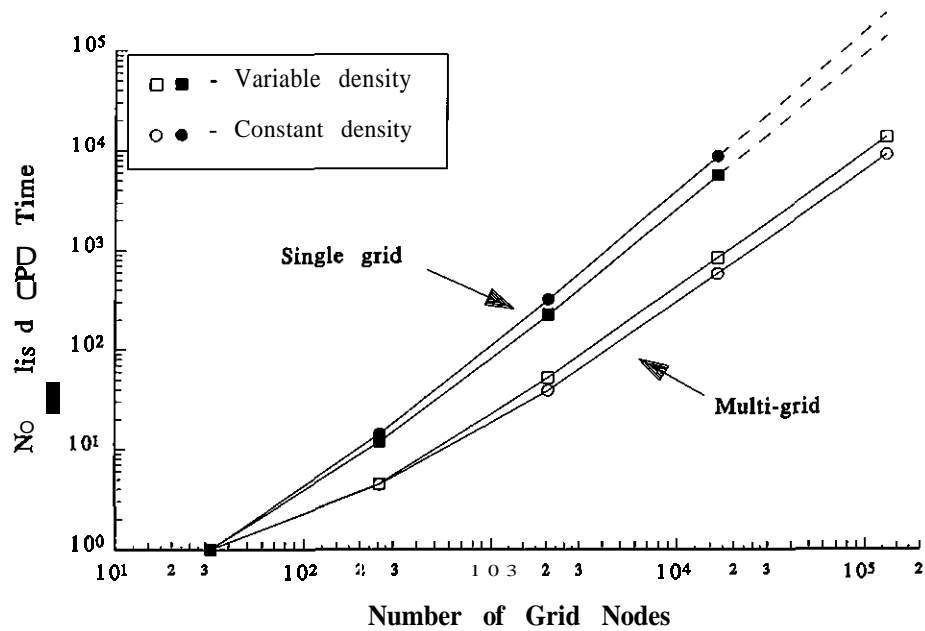


Fig. 7 Normalized computer time for convergence against grid density (squares, variable-density flow; circles, constant-density flow; open symbols, multigrid; filled symbols, single grid).

tended to embedded multigrid/multilevel calculations of practical engineering flows [20].

REFERENCES

1. W. P. Jones and J. H. Whitelaw, Calculation Methods for Turbulent Reacting Flows, *Combust. Flame*, vol. 48, 1982.
2. U. Ghia, K. N. Ghia, and C. T. Shin, High-Re Solutions for Incompressible Flow Using the Navier-Stokes Equations and a Multi-Grid Method, *J. Comput. Phys.*, vol. 19, pp. 387-411, 1975.
3. R. E. Phillips, T. F. Miller, and F. W. Schmidt, A Multilevel-Multigrid Algorithm for Axisymmetric Recirculating Flows, *Fifth Symp. Turbulent Shear Flows*, Cornell University, Ithaca, N.Y., pp. 20.21-20.25, 1985.
4. S. P. Vanka, Block-Implicit Multigrid Solution of Navier-Stokes Equations in Primitive Variables, *J. Comput. Phys.*, vol. 65, pp. 138-158, 1986.
5. S. Sivaloganathan and G. J. Shaw, A Multigrid Method for Recirculating Flows, *Int. J. Numer. Meth. Fluids*, vol. 8, pp. 417-440, 1988.
6. M. Barcus, M. Peric, and G. Scheuerer, Finite-Volume Multigrid Solutions of the Two-Dimensional Incompressible Navier-Stokes Equations, *Notes Numer. Fluid Mech.*, Vieweg, Braunschweig, vol. 23, pp. 37-47, 1988.
7. A. O. Demuren, Application of Multi-Grid Methods for Solving the Navier-Stokes Equations, *Proc. Inst. Mech. Eng.*, vol. 203, pp. 257-265, 1989.
8. A. Brandt, *Multigrid Techniques: 1984 Guide with Applications to Fluid Dynamics*, von Karman Inst. Lecture Ser. 194-04, pp. 1-183, 1984.
9. D. S. Joshi and S. P. Vanka, A Multigrid Calculation Procedure for Internal Flows in Complex Geometries, 28th Aerospace Sciences Meeting, Reno, Nevada, **AIAA-90-0442**, 1990.

10. C. M. Vaughan, S. Gilham, and J. W. Chew, Numerical Solutions of Rotating Disc Flows Using a Nonlinear Multigrid Algorithm, *Proc. 6th Int. Conf. Numerical Methods in Fluids*, Swansea, pp. 63-73, 1989.
11. J. W. Yokota, Diagonally Inverted Lower-Upper Factored Implicit Multigrid Scheme for the Three-Dimensional Navier-Stokes Equations, *AIAA J.*, vol. 29, no. 9, pp. 1642-1649, 1990.
12. M. Peric, M. Ruger, and G. Scheuerer, A Finite-Volume Multigrid Method for Calculating Turbulent Flows, *7th Symp. Turbulent Shear Flows*, Stanford University, Stanford, Calif., pp. 7.3.1-7.3.6, 1989.
13. B. E. Launder and D. B. Spalding, Numerical Computation of Turbulent Flows, *Comput. Meth. Appl. Mech. Eng.*, vol. 3, pp. 269-289, 1974.
14. A. Pollard and P. K. Yeung, Empirical Constants in the k - ϵ Model for Turbulent Channel Flow, Report No. TFG-90-1, Dept. Mech. Eng., Queen's University, Kingston, Ont. K7L 3N6, Canada.
15. G. J. Shaw and S. Sivaloganathan, On the Smoothing Properties of the SIMPLE Pressure Correction Algorithm, *Int. J. Numer. Meth. Fluids*, vol. 8, pp. 441-462, 1988.
16. S. V. Patankar, *Numerical Heat Transfer and Fluid Flow*, Hemisphere, Washington, D.C., 1980.
17. K. Stuben and G. Trottenberg, Multigrid Methods: Fundamental Algorithms, Model Problem Analysis, and Applications, in *Multigrid Methods, Lecture Notes in Mathematics*, vol. 960, Springer-Verlag, Heidelberg, 1982.
18. J. P. Van Doormaal and G. D. Raithby, Enhancements of the SIMPLE Method for Predicting Incompressible Fluid Flows, *Numer. Heat Transfer*, vol. 7, pp. 147-163, 1984.
19. B. R. Latimer and A. Pollard, Comparison of Pressure-Velocity Coupling Solution Algorithms, *Numer. Heat Transfer*, vol. 8, pp. 635-652, 1985.
20. P. A. Rubini and A. Pollard, An Embedded Multigrid/Multilevel Calculation Procedure for Three-Dimensional Variable-Density Turbulent Flows, Queen's University, Kingston, Ontario, in preparation.
21. S. P. Vanka, Block-Implicit Computation of Viscous Internal Flows—Recent Results, *AIAA* paper No. AIAA-87-0058, New York, 1987.
22. M. Matovic, A. Pollard, and P. Rubini, Evaluation of SIP and ADI Schemes for Three-Dimensional Turbulent Flows, Queen's University, Kingston, Ontario, in preparation.

Received 22 August 1991
Accepted 1 November 1991

Requests for reprints should be sent to A. Pollard.

Vertical line of text on the left margin.

Small mark or character in the center of the page.

Small mark or character in the bottom right corner.

Faint, illegible text or markings in the lower right quadrant.